HHS Public Access

Author manuscript

Prostate. Author manuscript; available in PMC 2022 November 01.

Published in final edited form as:

Prostate. 2021 November ; 81(15): 1202–1213. doi:10.1002/pros.24216.

MEX3D is an oncogenic driver in prostate cancer

Longjiang Shao, **Jianghua Wang**, **Omer Karatas**[1], **Michael Ittmann**

Dept. of Pathology & Immunology Baylor College of Medicine and Michael E. DeBakey Dept. of Veterans Affairs Medical Center, Houston, Texas 77030

Abstract

Background: Prostate cancer is the most common visceral malignancy and the second leading cause of cancer deaths in US men. The two most common genetic alterations in PCa are expression of the TMPRSS2/ERG (TE) fusion gene and loss of the PTEN tumor suppressor. These genetic alterations act cooperatively to transform prostatic epithelium but the exact mechanisms involved are unclear.

Methods: Microarray expression analysis of immortalized prostate epithelial cells transformed by loss of PTEN and expression of the TE fusion revealed MEX3D as one of the most highly upregulated genes. MEX3D expression in prostate cancer was examined in patient samples and in silico. In vitro and in vivo studies to characterize the biological impact of MEX3D were carried out. Analysis of the TCGA PanCancer database revealed TCF3 as a major target of MEX3D. The induction of TCF3 by MEX3D was confirmed and the biological impact of TCF3 examined by in vitro studies.

Results: MEX3D is expressed at increased levels in prostate cancer and is increased by decreased PTEN and/or expression of the TE fusion gene and drives soft agar colony formation, invasion and tumor formation in vivo. The known oncogenic transcription factor TCF3 is highly correlated with MEX3D in prostate cancer. MEX3D expression strongly induces TCF3, which promotes soft agar colony formation and invasion in vitro.

Conclusions: Loss of PTEN and expression of the TE fusion gene in prostate cancer strongly upregulates expression of MEX3D and its target TCF3 and promotes transformation associated phenotypes via this pathway.

Keywords

MEX3D; PTEN; TMPRSS2/ERG; TCF3; prostate cancer

Correspondence: Michael Ittmann MD/PhD, Department of Pathology & Immunology, Baylor College of Medicine, One Baylor Plaza Houston, TX 77030, Tele: (713) 798-6196, mittmann@bcm.edu.

[1]Current address: Dept. of Molecular Biology and Genetics Department, Erzurum Technical University, Erzurum, Turkey

Ethics Approval Statement: All animal procedures were carried out in accordance with Baylor College of Medicine ACUC approved procedures. Human tissue samples used in this study were obtained after informed consent under a Baylor College of Medicine Institutional Review Board approved protocol.

Conflicts of interest: The authors disclose no potential conflicts of interest.

INTRODUCTION

Prostate cancer (PCa) is the most common malignancy in American men, affecting one in nine men over 65 years of age. Currently there is no cure for the advanced stages of PCa and it is the second-leading cause of male cancer mortality. The TMPRSS2/ERG (TE) fusion gene is the most common genomic alteration in PCa and is present in approximately 50% of cases. This fusion results in high levels of TE fusion gene expression under the androgen regulated TMPRSS2 promoter. PCas with the TE fusion have been shown to have activation of multiple pathways which promote tumorigenesis[1–13]. Correlative studies in human prostate cancers reveal a frequent association of the TE fusion gene with loss of PTEN and studies in mouse models reveal that ERG expression and PTEN loss synergistically promote prostate cancer progression[14–17]. The mechanistic basis for the association of TE expression and PTEN loss is not clear.

In prior studies to determine the mechanistic basis of transformation induced by TE overexpression and/or PTEN loss we expressed the TE fusion gene and/or knocked down PTEN in the immortalized prostate epithelial cell line PNT1A[18]. Expression of the TE fusion alone or knockdown of PTEN increased proliferation and invasion but did not fully transform the PNT1A cells. However, TE fusion expression combined with PTEN knockdown resulted in acquisition of the ability to form colonies in soft agar and form tumors in SCID mice. Our initial studies identified activation of fibroblast growth factor (FGF) signaling as an important component in the transformation induced by TE fusion expression and PTEN loss. We have now identified MEX3D, a known oncogene, as another key downstream oncogenic activator in this context.

MATERIALS AND METHODS

Cell lines and tissue culture.

PNT1A cells were obtained from the European Type Culture Collection. LNCaP, DU145, VCaP and HEK293T cells were obtained from the American Type Culture Collection. Cell were obtained between 2001 and 2012, expanded, frozen and stored as stocks in liquid nitrogen. All cell lines are authenticated by STR analysis at MD Anderson Cancer Center Characterized Cell Line Core Facility. PNT1A, DU145 and LNCaP cells were maintained in the RPMI with 10% fetal bovine serum (FBS). VCaP and HEK293T cells were cultured in DMEM with 10% FBS. Cell numbers were determined with 0.4% Trypan Blue Solution using a Bio-Rad TC-20 automatic cell counter. All experiments were repeated at least three times. Cells were treated with the AKT kinase inhibitor AZD5363 as described previously[18]

Generation of stable cell lines.

PNT1A shMEX3D or VCaP-shMEX3D were generated by infecting with shMEX3D lentivirus. A total of 5 GIPZ MEX3D shRNA isoforms were obtained from the Baylor College of Medicine Cell Based Assay Screening Core: #1: V3LHS_307378, #2: _307380, #3: _634459, #4 _634464 and #5 _634465 and pGIPz noncoding vector. After transient transfection selection, the isoforms with the most efficient knockdown _634464 and _634465 and pGIPz non coding vector were used for lentivirus generation.

To construct the Myc-MEX3D construct, the human MEX3D ORF cDNA clone was purchased from Creative Biogene (NM_001174118.1, Cat# CDCR356960) in the pCDNA3.1(+) vector. To clone the MEX3D cDNA sequence into pCDH-CMV vector with a c-Myc tag,a primer set of MEX3D Exp F BstBI 5'- CTAG TT CG AA TGGGCAAGCCTATCCCTAAC −3' and MEX3D R Swa 1 5' CG ATTT AAAT CA GTA CTG TCT CTG CAG A GC G 3' was used to amplified the MEX3D fragment, and the amplicon was sub-cloned into a pCDH-CMV a vector with Myc tag using a Cold Fusion Cloning Kit from System Biosciences (Cat#MC010B-1. The MEX3D sequence was verified and MEX3D protein expression was confirmed by real time PCR and Western blotting with c-Myc-tag Ab (clone 9E10, Sigma). Flag-TCF3 plasmid was purchased from NovoPro, in which the cDNA/ORF sequence (NM_003200) in pcDNA3.1-3xFlag vector.

The PNT1A PTEN KD, TE, PTEN KD/TE and control cell lines were generated previously[18]. The shMEX3D lentiviruses described above were used to make the stable cell lines for VCaP-shMEX3D and PNT1A shMEX3D with puromycin selection (400 ng/mL for selection and 200 ng/mL for maintenance). Lentivirus for myc-MEX3D were generated using pCDH-CMV-myc-MEX3D and pPACK Lentivector packaging Kit (TR30037A) in 293T cells and infected into PNT1A cells to generate myc-MEX3D overexpressing cells. GFP positive cells for PNT1A were collected by FACS and used for in vitro and in vivo experiments.

siRNAs or plasmid DNA transfections.

Lipofectamine RNAiMAX was used for siRNA cell transfection experiments with 6 pmol RNAi duplex, mixed with Lipofectamine RNAiMAX (Thermo Scientific, # 13778150) in Opti-MEM I Reduced Serum Medium following the manufacturer's protocol. Cells were harvested 48 hours post transfection for cell proliferation or colony formation studies, or lysates collected for RNA or protein analysis. Human MEX3D siRNA duplexes (10 uM) were purchased from Santa Cruz with 3 different isoforms. The human TCF3 (E2A) siRNA, PTEN, TE fusion gene and control non-silencing siRNA scrambled sequences were purchased from Sigma. See Supplementary Table 1 for the siRNA sequences. In double transfections with plasmid and siRNA experiments, jetPRIME (Cat.# 114–15, Polyplus) was used. Briefly, cells were grown in 10 cm dishes and transfected with 10 μg DNA in 500 μl jetPRIME buffer with 20 μl of jetPRIME reagent, or 50 nM of siRNA duplex into 500 μl jetPRIME buffer with 20 μl of jetPRIME reagent. After 15 min incubation at room temperature, the transfection mixtures were added to the dishes with corresponding cells and placed in the incubator overnight. The next day, cells were trypsinized, counted for used to set up proliferation, invasion or soft agar colony formation assay.

Matrigel invasion assays.

Invasion assays were conducted using pre-coated BD Matrigel 8.0 uM Transwell Chamber 24 well plates (# 354480, BD Biosciences) in triplicate. A total of 24000 cells were added to each well after overnight transfection in 300 uL FBS free medium and 500 uL complete medium was added to the bottom in the 24 well plate. After 48 hours, membranes were fixed in neutral buffered formalin, stained with 0.05% crystal violet solution for 10 minutes and

mounted on a slide with EcoMount (Biocare #EM897L), sealed with coverslips and invasive cells counted. Each experiment was repeated 3 times.

Soft agar colony formation assays.

Briefly, shRNA infected stable cells or siRNA transfected cells 48 hrs after transfection were trypsinized and mixed (1000 cells /well) with the 0.7% agarose (top agar) with warm 2×RPMI 1640 with 20% FBS and plated in each well of 24 well plate on top of the prepared 1% base agar. Plates were incubated at 37°C for 15 to 20 days. Biweekly, 100 uL complete medium was added to keep the wells moist. At termination, the colonies were stained with 200 uL of p-iodonitrotetrazolium violet (2 mg/mL) overnight. The images were taken and colonies of 50 or more cells were counted.

cDNA Synthesis and Quantitative Real-time PCR.

Total RNA was isolated using the RNeasy Mini Kit (Qiagen) with RNase-Free DNase on-column digestion to remove the genomic DNA. 500 ng total RNA were used for cDNA reverse transcription using amfiRivert cDNA Synthesis Platinum Master Mix (Cat.# R5600, GenDEPOT). 1–5 ul of cDNA was used for Q-RT-CR in a final reaction volume of 15 ul using SYBR Green PCR Master Mix (Applied Biosystems) or TaqMan Fast Advanced Master Mix (Applied Biosystems) using ABI StepOne Plus Real-Time PCR system. The quantitative real-time PCR primers for PTEN, TCF3 and MEX3D-myc used are shown in Supplementary Table 1. Human MEX3D probe FAM-MGB qHsaCEP0054727 and β-Actin VIC-MGB were used for TaqMan QPCR. PTEN and MEX3D were analyzed using SYBR Green real time PCR with β-actin as input control. Each experiment was performed in triplicate and the differences in expression levels were evaluated using 2- ΔΔCT method. Expression data were normalized to β-actin.

Western blotting.

Cells were trypsinized and collected by centrifugation, and whole-cell lysates were obtained using a lysis buffer as described previously[18]. Total protein concentration was determined using a BioRad DC protein assay reagent. Aliquots containing 30 ug of total protein from each sample were prepared in Laemmli buffer, resolved on 4–15 % SDS-PAGE gels from Bio-Rad Mini-Protean TGX Gel and electrotransferred to nitrocellulose membranes using iBlot 2 Transfer Stacks system from Thermo Fisher Scientific. The LI-COR system was used for signal detection, in which LiCOR Odyssey Blocking Buffer(TBS, #927-50000) was used for blocking for 1 hour and primary antibody incubation overnight at 4°C followed by 5 washes with TBST buffer (Tris pH 7.4 with 0.1% Tween20). The blot was then incubated in secondary antibodies (goat anti mouse IRDye 680RD #925-68070 and goat anti Rabbit IRDye 800CW, 926-32211) were simultaneously, diluted in blocking buffer(1:15000) for 1 hour incubation at room temperature. After 5 washes the blots were scanned using LICOR Odyssey CLx. Imager with Image Studio version 5.2 for image acquisition and band density analysis according to the manufacture’s procedure.

Antibodies.

Myc-tag antibody (9E10) and Flag M2 antibody from Sigma were used for pull down experiments. For Western blotting, Myc and Flag antibodies were diluted as 1:5000, while Anti-TCF3 antibody (Abcam #ab82847), and anti- MEX3D antibody(Abcam #ab79208) were used as 1:1000 dilution in the LICOR blocking buffer supplemented with 2% Tween 20.

Co-immunoprecipitation.

All immunoprecipitation steps were carried out at 4°C. HEK293 cells were transfected with Myc-tagged MEX3D and Flag-tagged-TCF3 plasmid DNAs with Lipofectamine 2000 (Cat.#11668019, ThermoFisher), Cells were lysed in Pierce IP Lysis Buffer composed of 25 mM Tris-HCl pH 7.4, 150 mM NaCl, 1 mM EDTA, 1% NP-40 supplemented with 1 mM PMSF and 1X protease/phosphatase inhibitor (ThermoFisher Scientific). After clearing, 30 ul slurry of protein A/G-agarose (Santa Cruz Biotechnology) and 2 ug of the anti-Myc or anti-Flag or control IgG antibody were added to 1–2 mg of the extracted proteins and rotated for 16 hrs. Next, the beads were spun down at 500g for 1 min, and rinsed 4 times with washing buffer containing 25 mM Tris-HCl pH 8.0, 150 mM NaCl and 1 mM EDTA for 5 minutes each with rotation at 4°C. Finally, the beads were heated at 37 °C for 10 minutes and then 55 ° C for 6 minutes in 2X Laemmli buffer and Western blot performed.

Mouse xenografts.

SCID male mice at 7–9 weeks of age were injected subcutaneously in each flank with 3×10^6 PNT1A cells overexpressing Myc-MEX3D, Flag-TCF3 or PNT1A empty vector control cells in 50% Matrigel as described previously[18]. A total of 5 mice per group were used. Tumor formation was checked twice weekly for 14 weeks.

Prostate and prostate cancer tissues.

Tissue samples were obtained from the Human Tissue Acquisition and Pathology Core of the Dan L. Duncan Cancer Center and were collected from fresh radical prostatectomy specimens after obtaining informed consent under an Institutional Review Board approved protocol. Cancer samples contained a minimum of 70% cancer and benign tissues were free of cancer on pathological examination. RNAs were extracted using QIAGEN DNA/RNA Mini kit according to manufacturer's instruction

Statistical analysis.

The data were expressed as the means +/− SD of three or more independent experiments. Statistical analysis was performed using the two-tailed Student's t-test, Mann-Whitney or One-way ANOVA on Ranks as appropriate to compare numerical values. Correlations were assessed using Pearson Product Moment test. Proportions were compared using Fisher exact test. P values less than 0.05 were considered statistically significant.

RESULTS

MEX3D is an oncogene induced by the TE fusion gene and PTEN loss.

In our previous published studies[18] we established cell lines using the immortalized prostate epithelial cell line PNT1A with TE expression, PTEN knockdown (KD) or TE overexpression with PTEN knockdown (TE/PTEN KD). The three cell lines all showed phenotypic alterations such as increased proliferation and invasion relative to controls, but only the TE/PTEN KD cell line was fully transformed and capable of growing in soft agar and as xenografts in SCID mice[18]. Microarray analysis of gene expression in these cell lines identified 260 protein encoding genes that were upregulated 1.4-fold or greater only in the TE/PTEN KD cell line[18]. Among these genes, the second most upregulated gene was MEX3D, which was upregulated 3.6 fold. This gene attracted our interest since it had been identified as a gene that may contribute to androgen independent growth in PCa based on a lentiviral mutagenesis screen[19].

Initially we sought to confirm the changes in gene expression observed on the microarrays by Q-RT-PCR. As seen in Figure 1A, MEX3D was increased in TE cells (1.2 fold), more significantly increased in PTEN KD cells (1.7 fold) and showed the highest increase in TE/PTEN KD cells (2.6 fold), confirming the results of our microarray studies. Treatment of TE/PTEN KD cells with the AKT kinase inhibitor AZD5363 significantly decreased MEX3D mRNA (Figure 1B). To confirm the induction of MEX3D by the TE fusion we transiently transfected the TE fusion cDNA into PNT1A cells using increasing amounts of plasmid and observed a proportional increase in MEX3D expression compared to control plasmid (Figure 1C). In PCa cells, knockdown of PTEN in either VCaP or DU145 cells (both PTEN wild type) increased MEX3D mRNA (Figure 1D). Finally, we confirmed these observations in VCaP cells at the protein level using quantitative Western blotting. As shown in Figure 1E, transient knockdown of PTEN increased MEX3D protein while knockdown of TE fusion gene in the context of PTEN knockdown markedly diminished the increase in MEX3D protein. These results confirm that MEX3D is a direct or indirect downstream target of the PI3K/PTEN/AKT pathway and the TE fusion gene and is potently induced by a combination of TE expression and PTEN knockdown.

To examine whether MEX3D is increased in PCa, we measured expression of MEX3D mRNA by Q-RT-PCR in RNAs from 37 PCa tissue samples and matched benign prostate tissue from radical prostatectomies. MEX3D was significantly increased in PCa ($P<.001$, t-test; Fig 2A). We then examined expression of MEX3D mRNA in existing datasets on Oncomine (Fig 2B). In the PCa datasets with MEX3D mRNA data, 5 of 7 showed significantly increased MEX3D expression in cancer relative to benign tissue ($p\leq.01$). Examination of MEX3D, PTEN and ERG in the TCGA data set showed that ERG was overexpressed and PTEN was lost in a significantly higher fraction of cases with high MEX3D compared to cases with unaltered MEX3D expression (Fig 2C). Conversely, ERG and PTEN were unaltered in a significantly lower fraction of cases without MEX3D overexpression compared to cases with high expression, consistent with our in vitro observations. Western blotting revealed VCaP and LNCaP express significantly more MEX3D protein than PNT1A cells, while 22RV1, PC3 and LAPC4 express somewhat

higher levels. Of note, VCaP cells express the TE fusion gene while LNCaP have a mutated PTEN. DU145 cells did not express detectable MEX3D protein (Fig 2D) and have wild type PTEN and do not have a TE fusion gene. Thus, PCa cell lines express variable, but generally increased, levels of MEX3D protein compared to benign prostate epithelial cells. MEX3D was also very significantly increased in variety of malignancies including colorectal cancer, glioblastoma, melanoma, high-grade sarcoma (Supplementary Fig 1) and many other malignancies.

To determine the biological significance of MEX3D expression, we used siRNA to knock down MEX3D or TE fusion gene and the ability to form colonies in soft agar was assessed. Colony formation was markedly decreased by MEX3D knockdown. TE knockdown was performed as a positive control and it also resulted in significant decrease in soft agar colony formation. To determine the relevance of MEX3D in PCa cell lines we analyzed the impact of MEX3D knockdown with siRNA on soft agar colony formation in VCaP cells. PTEN is not altered in VCaP cells and there are no known alterations in the PI3K pathway in these cells, which are also the only cell line known to express the TE fusion gene. Knockdown of MEX3D significantly decreased colony formation in VCaP cells ($p<.001$, t-test; Fig 3B). As expected, knockdown of PTEN with siRNA increased soft agar colony formation in VCaP cells ($p<.001$). Knockdown of PTEN in VCaP cells with MEX3D knockdown increased colony formation slightly but significantly compared to MEX3D knockdown only ($p=.048$, Mann-Whitney). Overall, these results indicate that MEX3D plays an important role in the increased soft agar colony formation induced by PTEN knockdown in this context. We also examined the impact of MEX3D on invasion. As shown in Figure 3C, MEX3D expression increased invasion while MEX3D knockdown decreased invasion of PNT1A cells, showing MEX3D is a cell invasion stimulator. Finally, MEX3D overexpressing PNT1A cells formed tumors in SCID mice in 6 of 10 injections after 14 weeks while vector control cells formed no tumors. Thus, MEX3D is an oncogene with full transforming activity in prostate epithelial cells.

TCF3 is upregulated by MEX3D expression

To discover potential downstream targets of MEX3D that could mediate its oncogenic activity, we examined the TCGA PanCancer Atlas prostate cancer database mRNA expression data in cBioportal[20]. The gene most strongly correlated with MEX3D is TCF3, which has a very strong correlation (.64, q-value 1.1×10^{-52}, Fig 4A). Other large PCa databases with mRNA data from primary or metastatic cancers also showed extremely high correlation of TCF3 with MEX3D (Figure 4B). Examination of all the tumor types in the PanCancer Atlas showed very strong positive correlation of TCF3 with MEX3D mRNA in 27 of 32 tumor types (Supplementary Table 2). Based on our in vitro experiments, we would predict a negative correlation of MEX3D and PTEN expression in PCa in addition to the strong positive correlation with TCF3. Examination of the correlation of PTEN and MEX3D expression showed strong negative correlation in the two primary PCa databases (TCGA and MSKCC) but not in the SU2C metastatic database (Figure 4B). It should be noted that the PI3K/AKT pathway is activated by many different genetic alterations in advanced prostate cancer[21], which would obscure a potential correlation with decreased PTEN mRNA expression.

These findings were of considerable interest since TCF3 is a bHLH transcription factor that is a part of several fusion oncogenes in acute leukemias[22]. In addition, it has been shown to have oncogenic activities in vitro in a variety of malignancies including prostate[23,24], esophageal[25] and breast cancer[26], glioblastoma[27] and chronic lymphocytic leukemia[28]. Increased expression of TCF3 is associated with adverse outcome in a number of cancers[29–32]. Examination of Oncomine databases revealed increased expression of TCF3 in prostate cancer compared to benign prostate ($p<.01$) in 9 of 16 databases (including all of the databases with increased MEX3D; examples in Fig 4C). TCF3 is also increased in many other malignancies including colon cancer, glioblastoma, melanoma and high grade sarcoma, which also have increased MEX3D (Fig 4D). Of note, TCF3 is increased in several cancers without significantly increased levels of MEX3D, such leukemia and breast carcinoma, implying that MEX3D may be one of several factors regulating TCF3 in cancer.

Based on these observations we examined the regulation of TCF3 mRNA by MEX3D. Transfection of LNCaP cells with Myc-tagged MEX3D plasmid resulted in a marked increase in TCF3 mRNA expression. The converse experiment revealed a marked upregulation of MEX3D mRNA by Flag-tagged TCF3 transfection (data not shown). These results suggest a very strong cross regulation of TCF3 and MEX3D at the mRNA level. We therefore examined this cross regulation at the protein level in 293 cells. Transfection of Myc-tagged MEX3D into 293 cells strongly induces expression of TCF3 (Fig 5A). In the converse experiment, transfection of a Flag-tagged TCF3 strongly induced MEX3D in 293 cells (Fig 5B). In both experiments, there was a strong linear correlation of protein expression of TCF3 and MEX3D ($r=.97$ and .94, respectively). A similar strong induction of TCF3 protein was seen in VCaP PCa cells when they were transfected with Myc-tagged MEX3D (Fig 5C).

To determine if TCF3 and MEX3D proteins interact with each other, we carried out cotransfection with Myc-tagged MEX3D and Flag-tagged TCF3 in 293 cells and then carried out immunoprecipitation with anti-Myc, anti-Flag or control IgG. Co-immunoprecipitation of the tagged proteins was seen using both anti-Myc and anti-Flag antibodies (Fig 5D), demonstrating the interaction of the MEX3D and TCF3 proteins.

TCF3 is an oncogene in prostate epithelium and mediates MEX3D oncogenic activity

To determine the biological significance of TCF3 expression in prostate cells we established PNT1A cell overexpressing TCF3. As shown in Fig 6A, these cells formed colonies in soft agar, while control PNT1A cells did not, although the colony formation was lower than PNT1A cells expressing MEX3D (Fig 6A). Knockdown of TCF3 in PNT1A cells expressing MEX3D markedly decreased both soft agar colony formation (Fig 6A) and invasion (Fig 6B). The TCF3 expressing PNT1A cells did not form tumors in SCID mice (data not shown). Thus TCF3 has oncogenic activity in prostate epithelial cells but is not fully transforming.

DISCUSSION

Loss of PTEN expression is one of the most common molecular alterations in prostate cancer and is strongly associated with progression. Expression of the TE fusion gene is

present in approximately half of all prostate cancers and is associated with loss of PTEN expression. In our current studies, we have identified MEX3D as a novel oncogene that is induced by PTEN loss and to a lesser extent expression of the TE fusion gene. MEX3D expression is increased in prostate cancer and in vitro studies indicate that it enhances soft agar colony formation and invasion. When inoculated into immunodeficient mice, PNT1A cells over-expressing MEX3D were tumorigenic in 6 of 10 injections, while controls showed no tumors. Thus, MEX3D can fully induce cell transformation. MEX3D was previously identified as a potential inducer of androgen independent growth in insertional mutagenesis screen and our studies are consistent with this finding[19]. Interestingly, MEX3D is overexpressed in a number of other malignancies suggesting it may have oncogenic properties in a variety of cellular contexts although this has not been tested directly. In these other malignancies expression of MEX3D may be induced loss of PTEN (i.e. glioblastomas) or other alterations increasing the PI3K/AKT pathway or perhaps other ETS transcription factors. Of course, other, as yet unknown genetic or epigenetic alterations may play a role in increased MEX3D expression in other cancers.

The function of the MEX3D gene is poorly characterized. It was originally described as a member of MEX3 gene family[33] (MEX3A-D). The original description of these genes focused on MEX3A-C, which were shown to be RNA binding proteins. MEX3A-C have all been shown to be RNA binding E3 ubiquitin ligases that can mediate protein, and in some cases, RNA degradation[34–38]. MEX3A, B and/or C have all been previously implicated as oncogenes in a several cancers including gastric[35,39] and bladder cancer[40] and glioblastoma[34]. Importantly, MEX3B and MEX3C can mediate resistance in cancer immunotherapy by mediating degradation of MHC proteins[41–43]. Whether MEX3D has similar activities is unknown.

Our studies identify the TCF3 transcription factor as a major downstream target of MEX3D in PCa. Expression of MEX 3D is very highly correlated with TCF3 expression in prostate and many other cancers. Our in vitro studies indicate that they strongly cross regulate each other at the mRNA level. This could be due to transcriptional regulation or potentially post-transcriptional regulation such as increased RNA stability. In addition, it should be noted that MEX3D and TCF3 are located very near each other on chromosome 19p13.3 and so part of their correlation could be related to factors controlling transcription of this entire region. As predicted, knockdown of TCF3 attenuates MEX3D induced cancer phenotypes including colony formation and invasion in PNT1A cells overexpressing MEX3D.

TCF3 is a known oncogene that plays an important role in a subset of acute leukemias[22]. Studies have also implicated TCF3 as an oncogene in breast[26] and cervical cancers[31] and glioblastoma[27]. In breast cancer it is expressed particularly in the basal subtype and is associated with activation of a subset of Wnt target genes. In PCa cells, TCF3 is androgen induced and knockdown of TCF3 in DU145 and PC3 cells decreases proliferation and increases apoptosis[23]. As noted above, MEX3D can drive androgen independent growth. Our findings suggest a novel androgen receptor independent mechanism by which PI3K/AKT activation can promote androgen independent growth via MEX3D and TCF3 which it might constitute a novel target in PCa. In addition, TCF3 can enhance resistance to chemotherapy in PCa[24].

In summary, we have identified MEX3D as an oncogene in PCa that is induced by PTEN loss and TE fusion gene expression. Its oncogenic activities are mediated in part by induction of TCF3. Further studies are needed to understand how TCF3 is induced by MEX3D, the targets of TCF3 in PCa and whether the MEX3D has other targets in PCa that also contribute to its oncogenic activities.

Supplementary Material

Refer to Web version on PubMed Central for supplementary material.

Funding Statement:

This work was supported by grants from DOD Prostate Cancer Research Program (W81XWH-13-1-0367; MI), the Prostate Cancer Foundation (MI) and the National Cancer Institute to the Dan L. Duncan Cancer (P30 CA125123) supporting the Integrated Biospecimen Shared Resource and by the use of the facilities of the Michael E. DeBakey VAMC.

Data Availability:

Data is available upon request

REFERENCES

1. Vainio P, Lehtinen L, Mirtti T, et al.Phospholipase PLA2G7, associated with aggressive prostate cancer, promotes prostate cancer cell migration and invasion and is inhibited by statins. Oncotarget. 2011;2(12):1176–1190. [PubMed: 22202492]
2. Massoner P, Kugler KG, Unterberger K, et al.Characterization of transcriptional changes in ERG rearrangement-positive prostate cancer identifies the regulation of metabolic sensors such as neuropeptide Y. PLoS One. 2013;8(2):e55207. [PubMed: 23390522]
3. Cai C, Wang H, He HH, et al.ERG induces androgen receptor-mediated regulation of SOX9 in prostate cancer. The Journal of clinical investigation. 2013;123(3):1109–1122. [PubMed: 23426182]
4. Magistroni V, Mologni L, Sanselicio S, et al.ERG deregulation induces PIM1 overexpression and aneuploidy in prostate epithelial cells. PLoS One. 2011;6(11):e28162. [PubMed: 22140532]
5. Sun C, Dobi A, Mohamed A, et al.TMPRSS2-ERG fusion, a common genomic alteration in prostate cancer activates C-MYC and abrogates prostate epithelial differentiation. Oncogene. 2008;27(40):5348–5353. [PubMed: 18542058]
6. Wu L, Zhao JC, Kim J, Jin HJ, Wang CY, Yu J. ERG is a critical regulator of Wnt/LEF1 signaling in prostate cancer. Cancer research. 2013;73(19):6068–6079. [PubMed: 23913826]
7. Gupta S, Iljin K, Sara H, et al.FZD4 as a mediator of ERG oncogene-induced WNT signaling and epithelial-to-mesenchymal transition in human prostate cancer cells. Cancer Res. 2010;70(17):6735–6745. [PubMed: 20713528]
8. Yu J, Mani RS, Cao Q, et al.An integrated network of androgen receptor, polycomb, and TMPRSS2-ERG gene fusions in prostate cancer progression. Cancer Cell. 2010;17(5):443–454. [PubMed: 20478527]
9. Tomlins SA, Laxman B, Varambally S, et al.Role of the TMPRSS2-ERG gene fusion in prostate cancer. Neoplasia. 2008;10(2):177–188. [PubMed: 18283340]
10. Brase JC, Johannes M, Mannsperger H, et al.TMPRSS2-ERG -specific transcriptional modulation is associated with prostate cancer biomarkers and TGF-beta signaling. BMC Cancer. 2011;11:507. [PubMed: 22142399]
11. Tian TV, Tomavo N, Huot L, et al.Identification of novel TMPRSS2:ERG mechanisms in prostate cancer metastasis: involvement of MMP9 and PLXNA2. Oncogene. 2013.
12. Wang J, Cai Y, Shao LJ, et al.Activation of NF-{kappa}B by TMPRSS2/ERG Fusion Isoforms through Toll-Like Receptor-4. Cancer Res. 2011;71(4):1325–1333. [PubMed: 21169414]

13. Zhang L, Shao L, Creighton CJ, et al.Function of phosphorylation of NF-kB p65 ser536 in prostate cancer oncogenesis. Oncotarget. 2015.
14. King JC, Xu J, Wongvipat J, et al.Cooperativity of TMPRSS2-ERG with PI3-kinase pathway activation in prostate oncogenesis. Nature genetics. 2009;41(5):524–526. [PubMed: 19396167]
15. Han B, Mehra R, Lonigro RJ, et al.Fluorescence in situ hybridization study shows association of PTEN deletion with ERG rearrangement during prostate cancer progression. Mod Pathol. 2009;22(8):1083–1093. [PubMed: 19407851]
16. Leinonen KA, Saramaki OR, Furusato B, et al.Loss of PTEN is associated with aggressive behavior in ERG-positive prostate cancer. Cancer epidemiology, biomarkers & prevention : a publication of the American Association for Cancer Research, cosponsored by the American Society of Preventive Oncology. 2013;22(12):2333–2344.
17. Chen Y, Chi P, Rockowitz S, et al.ETS factors reprogram the androgen receptor cistrome and prime prostate tumorigenesis in response to PTEN loss. Nature medicine. 2013.
18. Shao L, Wang J, Karatas OF, et al.Fibroblast growth factor receptor signaling plays a key role in transformation induced by the TMPRSS2/ERG fusion gene and decreased PTEN. Oncotarget. 2018;9(18):14456–14471. [PubMed: 29581856]
19. Schinke EN, Bii V, Nalla A, et al.A novel approach to identify driver genes involved in androgen-independent prostate cancer. Mol Cancer. 2014;13:120. [PubMed: 24885513]
20. Cerami E, Gao J, Dogrusoz U, et al.The cBio cancer genomics portal: an open platform for exploring multidimensional cancer genomics data. Cancer Discov. 2012;2(5):401–404. [PubMed: 22588877]
21. Robinson D, Van Allen EM, Wu YM, et al.Integrative clinical genomics of advanced prostate cancer. Cell. 2015;161(5):1215–1228. [PubMed: 26000489]
22. Paulsson K, Jonson T, Ora I, Olofsson T, Panagopoulos I, Johansson B. Characterisation of genomic translocation breakpoints and identification of an alternative TCF3/PBX1 fusion transcript in t(1;19)(q23;p13)-positive acute lymphoblastic leukaemias. Br J Haematol. 2007;138(2):196–201. [PubMed: 17593026]
23. Patel D, Chinaranagari S, Chaudhary J. Basic helix loop helix (bHLH) transcription factor 3 (TCF3, E2A) is regulated by androgens in prostate cancer cells. Am J Cancer Res. 2015;5(11):3407–3421. [PubMed: 26807321]
24. Patel D, Chaudhary J. Increased expression of bHLH transcription factor E2A (TCF3) in prostate cancer promotes proliferation and confers resistance to doxorubicin induced apoptosis. Biochem Biophys Res Commun. 2012;422(1):146–151. [PubMed: 22564737]
25. Ma J, Wang XB, Li R, et al.RNAi-mediated TCF-3 gene silencing inhibits proliferation of Eca-109 esophageal cancer cells by inducing apoptosis. Biosci Rep. 2017;37(6).
26. Slyper M, Shahar A, Bar-Ziv A, et al.Control of breast cancer growth and initiation by the stem cell-associated transcription factor TCF3. Cancer Res. 2012;72(21):5613–5624. [PubMed: 23090119]
27. Li R, Li Y, Hu X, Lian H, Wang L, Fu H. Transcription factor 3 controls cell proliferation and migration in glioblastoma multiforme cell lines. Biochem Cell Biol. 2016;94(3):247–255. [PubMed: 27105323]
28. Kardava L, Yang Q, St Leger A, et al.The B lineage transcription factor E2A regulates apoptosis in chronic lymphocytic leukemia (CLL) cells. Int Immunol. 2011;23(6):375–384. [PubMed: 21551245]
29. Li C, Cai S, Wang X, Jiang Z. Hypomethylation-associated up-regulation of TCF3 expression and recurrence in stage II and III colorectal cancer. PLoS One. 2014;9(11):e112005. [PubMed: 25375219]
30. Huang A, Zhao H, Quan Y, Jin R, Feng B, Zheng M. E2A predicts prognosis of colorectal cancer patients and regulates cancer cell growth by targeting miR-320a. PLoS One. 2014;9(1):e85201. [PubMed: 24454819]
31. Luo L, Zhang H, Nian S, et al.Up-regulation of Transcription Factor 3 Is Correlated With Poor Prognosis in Cervical Carcinoma. Int J Gynecol Cancer. 2017;27(7):1422–1430. [PubMed: 28604457]

32. Shen X, Yuan J, Zhang M, et al.The increased expression of TCF3 is correlated with poor prognosis in Chinese patients with nasopharyngeal carcinoma. Clin Otolaryngol. 2017;42(4):824–830. [PubMed: 28107608]
33. Buchet-Poyau K, Courchet J, Le Hir H, et al.Identification and characterization of human Mex-3 proteins, a novel family of evolutionarily conserved RNA-binding proteins differentially localized to processing bodies. Nucleic acids research. 2007;35(4):1289–1300. [PubMed: 17267406]
34. Bufalieri F, Caimano M, Lospinoso Severini L, et al.The RNA-Binding Ubiquitin Ligase MEX3A Affects Glioblastoma Tumorigenesis by Inducing Ubiquitylation and Degradation of RIG-I. Cancers (Basel). 2020;12(2).
35. Xue M, Chen LY, Wang WJ, et al.HOTAIR induces the ubiquitination of Runx3 by interacting with Mex3b and enhances the invasion of gastric cancer cells. Gastric Cancer. 2018;21(5):756–764. [PubMed: 29417297]
36. Kuniyoshi K, Takeuchi O, Pandey S, et al.Pivotal role of RNA-binding E3 ubiquitin ligase MEX3C in RIG-I-mediated antiviral innate immunity. Proceedings of the National Academy of Sciences of the United States of America. 2014;111(15):5646–5651. [PubMed: 24706898]
37. Yoon JH, Abdelmohsen K, Kim J, et al.Scaffold function of long non-coding RNA HOTAIR in protein ubiquitination. Nature communications. 2013;4:2939.
38. Yoon JH, Abdelmohsen K, Kim J, et al.Scaffold function of long non-coding RNA HOTAIR in protein ubiquitination. Nat Commun. 2013;4:2939. [PubMed: 24326307]
39. Jiang H, Zhang X, Luo J, et al.Knockdown of hMex-3A by small RNA interference suppresses cell proliferation and migration in human gastric cancer cells. Mol Med Rep. 2012;6(3):575–580. [PubMed: 22692246]
40. Chao H, Deng L, Xu F, et al.MEX3C regulates lipid metabolism to promote bladder tumorigenesis through JNK pathway. Onco Targets Ther. 2019;12:3285–3294. [PubMed: 31118679]
41. Cano F, Bye H, Duncan LM, et al.The RNA-binding E3 ubiquitin ligase MEX-3C links ubiquitination with MHC-I mRNA degradation. Embo J. 2012;31(17):3596–3606. [PubMed: 22863774]
42. Cano F, Lehner PJ. A novel post-transcriptional role for ubiquitin in the differential regulation of MHC class I allotypes. Molecular immunology. 2013;55(2):135–138. [PubMed: 23140835]
43. Huang L, Malu S, McKenzie JA, et al.The RNA-binding Protein MEX3B Mediates Resistance to Cancer Immunotherapy by Downregulating HLA-A Expression. Clin Cancer Res. 2018;24(14):3366–3376. [PubMed: 29496759]

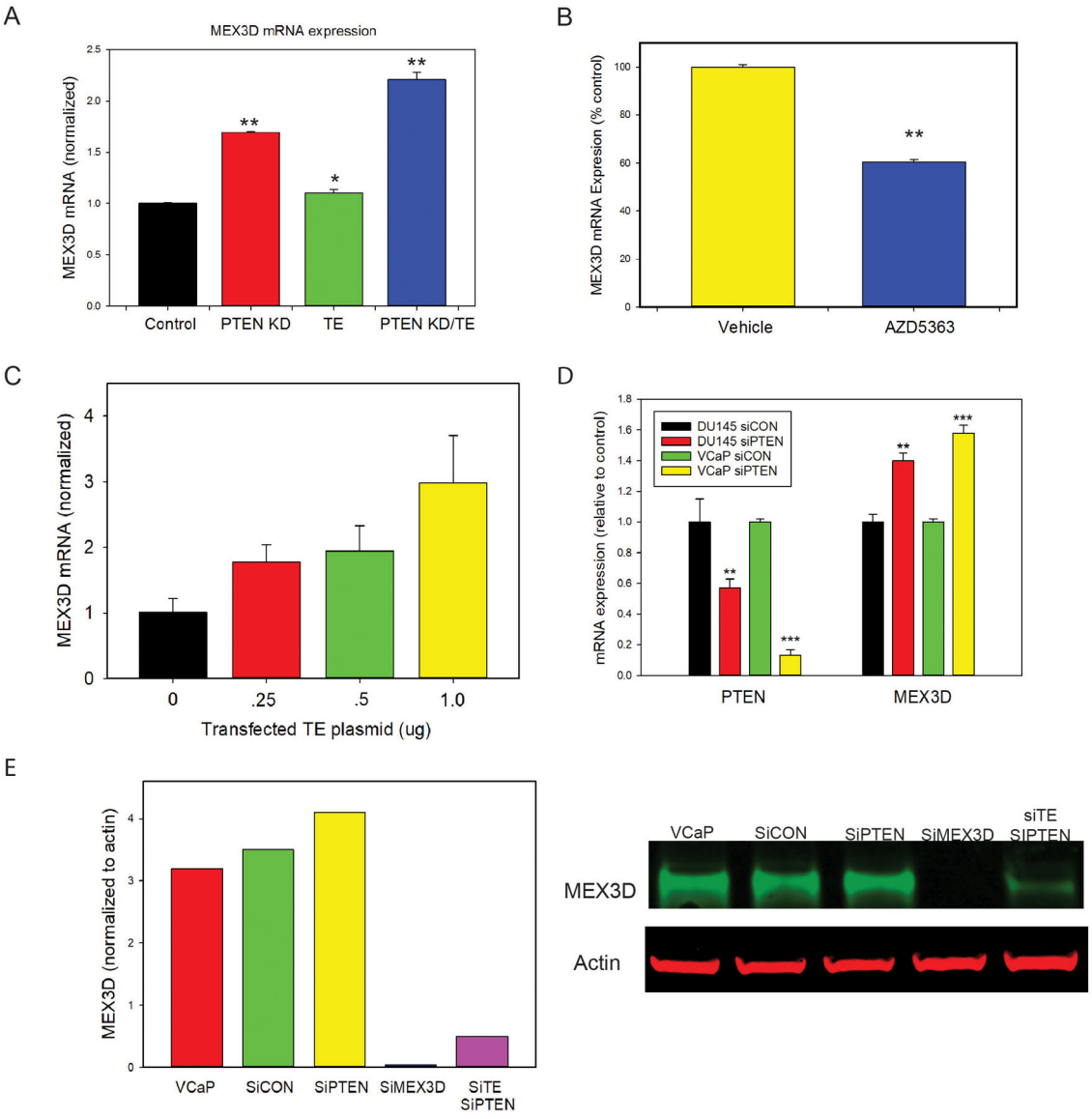

Figure 1. MEX3D expression is increased by AKT activity and TE fusion gene expression

A. Stable cell lines were established from PNT1A immortalized human prostate epithelial cells with knockdown of PTEN (PTEN KD), overexpression of the TMPRSS2/ERG fusion gene (TE) or with both fusion gene overexpression and PTEN knockdown (TE/PTEN KD). Expression of MEX3D mRNA as determined by Q-RT-PCR normalized to control cells is shown (mean +/− SD). Statistically significant increases in expression by t-test are indicated: * p<.05; ** p<.01

B. PTEN KD/TE cells were treated with the AKT kinase inhibitor AZD5363 or vehicle only and MEX3D mRNA quantitated by Q-RT-PCR. Means +/−SDs are shown. The decrease in expression was statistically significantly decreased by t-test; ** p<.01

C. PNT1A cells were transiently transfected with TE fusion expressing plasmid (.25, .5 or 1 ug) or control plasmid in triplicate and MEX3D mRNA measured after extraction by

Q-RT-PCR. Means +/− SD are shown. TE transfected cells had statistically significantly higher MEX3D mRNA than controls (ANOVA, p=.004).

D. DU145 and VCAP prostate cancer cells lines were transfected with siRNA targeting PTEN or control siRNA and levels of PTEN and MEX3D mRNA analyzed by Q-RT-PCR. Means +/−SDs are shown. The induction of MEX3D expression by PTEN knockdown was statistically significantly as determined by t-test; ** p<.01; *** p<.001

E. Quantitative Western blotting of VCAP cells transiently transfected with control siRNA, PTEN targeted siRNA, MEX3D targeted siRNA or both TE and PTEN targeted siRNAs. Quantitaive analysis of expression of MEX3D protein normalized to actin was then performed (left) after Western blotting (right).

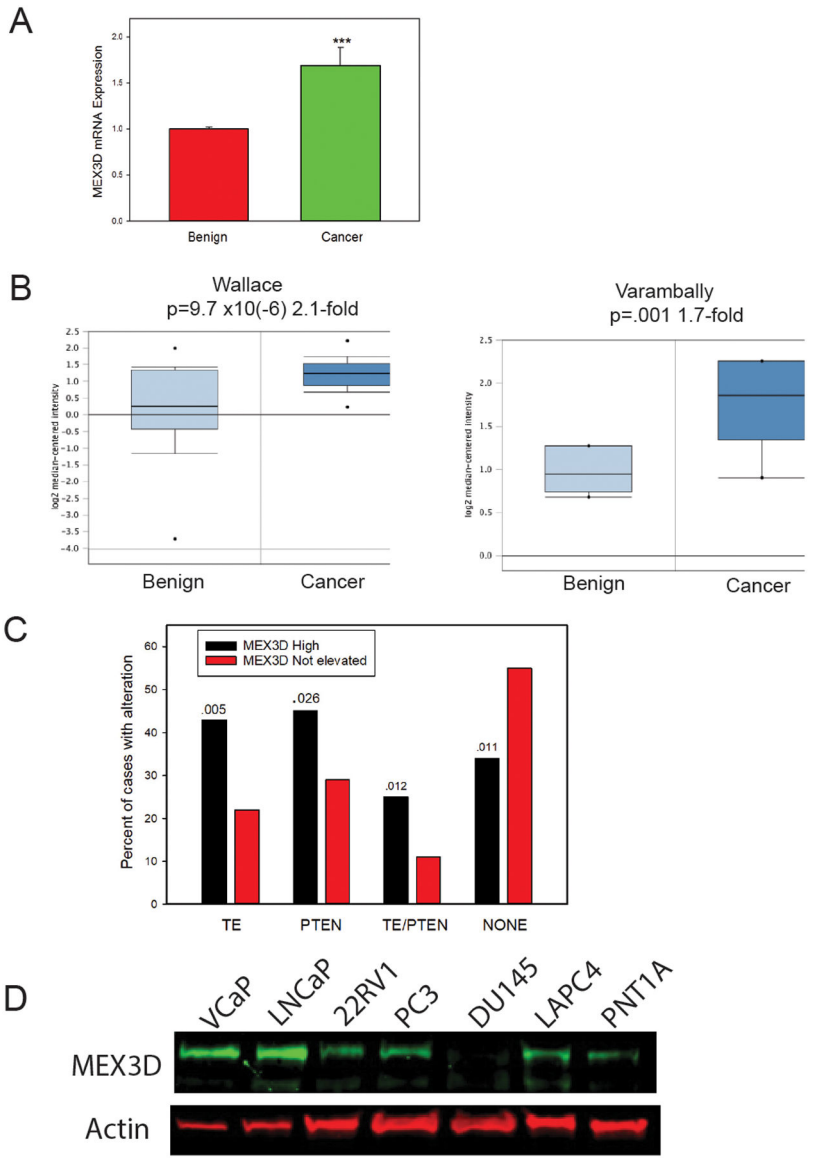

Figure 2. Increased expression of MEX3D in prostate cancer

A. Expression of MEX3D in mRNAs from 37 clinically localized prostate cancers and adjacent benign tissues as determined by Q-RT-PCR. Mean +/−SD shown. The increase in expression in prostate cancer was statistically significantly as determined by t-test (*** p<.001)

B. Examples of increased MEX3D expression in prostate cancer in Oncomine datasets. Box and whisker plot of log2 median centered intensity of benign and cancer tissue. The name of the database, p-value and fold change are shown.

C. The TCGA prostate cancer database (PanCancer) was analyzed for ERG, PTEN and MEX3D expression in cBioportal and cases with increased or decreased expression (1.4 fold) identified. Cases were divided into those with increased MEX3D or those with unaltered MEX3D expression. The fraction of cases in these two groups with ERG overexpression, decreased PTEN expression, both increased ERG and decreased PTEN

or no alterations in ERG or PTEN were determined. Statistical analysis of differences in the fraction altered for each comparison were determined by Fisher exact test; all were statistically different with p-values as shown.

D. Expression of MEX3D by Western blot of prostate cancer and immortalized prostate epithelial cells (PNT1A). Actin loading control is shown.

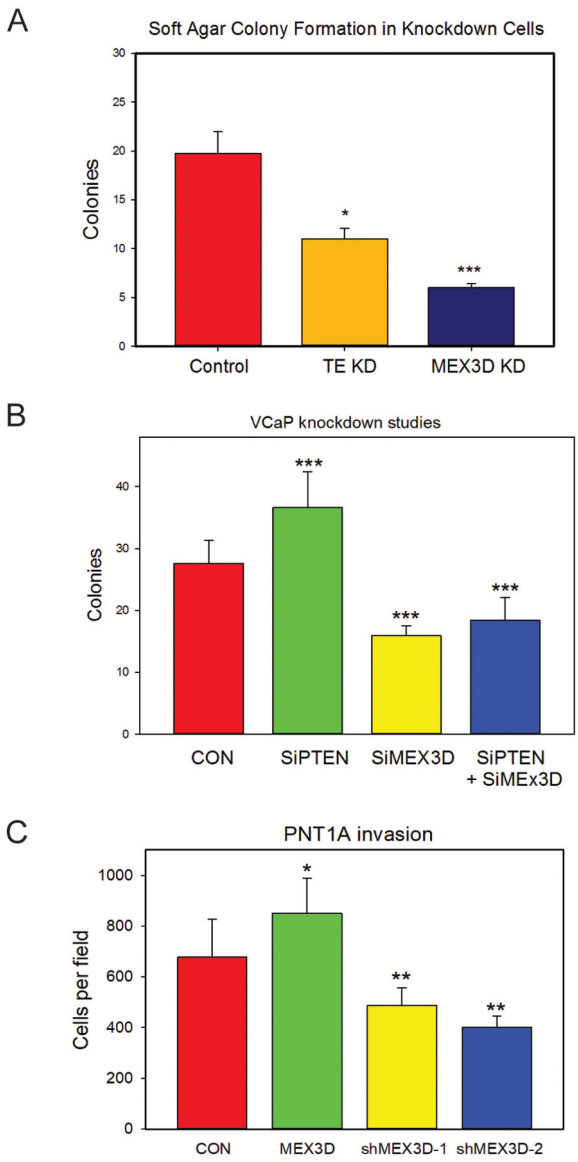

Figure 3. MEX3D has oncogenic activities in prostate cancer

A. Soft agar colony formation of TE/PTEN KD cells with knockdown the TE fusion gene or MEX3D or with control siRNA. Mean +/− SD. p<.05; *** p<.001 versus control; t-test

B. Soft agar colony formation in VCaP prostate cancer cells with control siRNA or with knockdown of PTEN, MEX3D or both PTEN and MEX3D. Mean +/− SD is shown. *** p<.001, t-test versus control

C. Matrigel invasion in PNT1A cells with MEX3D overexpression or knockdown of MEX3D. Mean +/− SD. p<.05; ** p<.01 versus control; t-test.

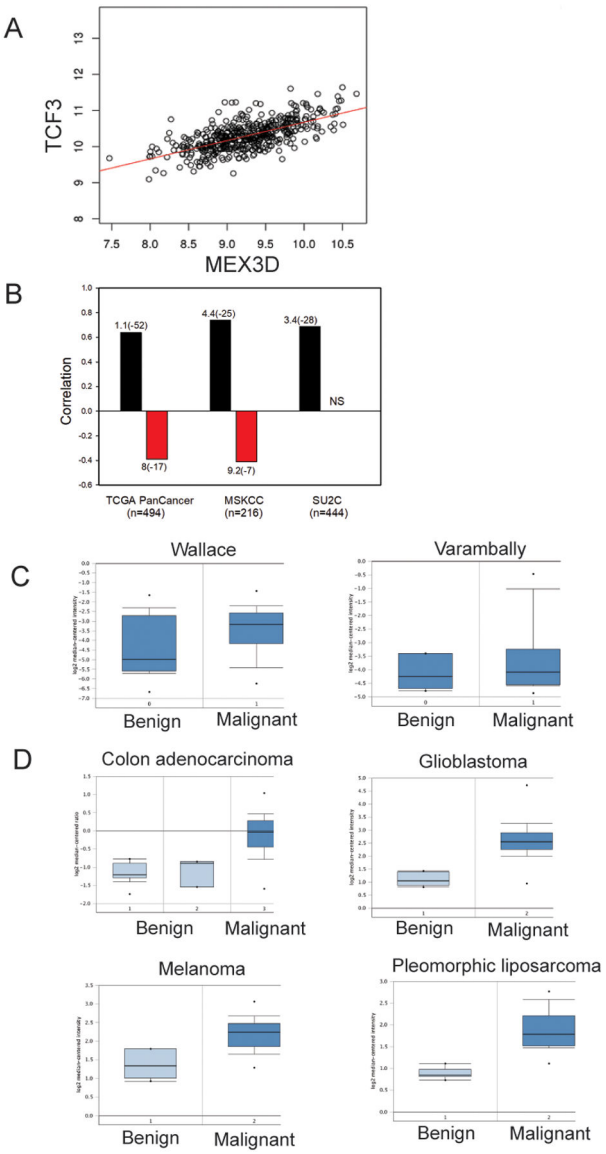

Figure 4. TCF3 is highly correlated with MEX3D and increased in prostate cancer

A. Correlation of TCF3 and MEX3D mRNAs in TCGA PanCancer Atlas primary prostate cancer database.

B. Correlation of MEX3D and TCF3 (black) and PTEN (red) in three large prostate cancer databases TCGA, Memorial Sloan Kettering (primary) and SU2C (metastatic). Q-values are shown over each bar showing correlation

C. Expression of TCF3 in benign prostate and prostate cancer in Oncomine databases. Wallace: 1.9 fold, p=.009; Varambally: 1.6 fold; $p= 3 \times 10^{-4}$

D. Expression of TCF3 in malignant tumors and corresponding benign tissues in Oncomine databases. Colon adenocarcinoma (TCGA): 2 fold, $p=1.5 \times 10^{-20}$; glioblastoma (TCGA): 2.8 fold, $p=1.1 \times 10^{-9}$; melanoma: Talantov 1.85 fold, $p=4.7 \times 10^{-3}$; pleomorphic liposarcoma: Barretina 1.96 fold, 1.3×10^{-10}

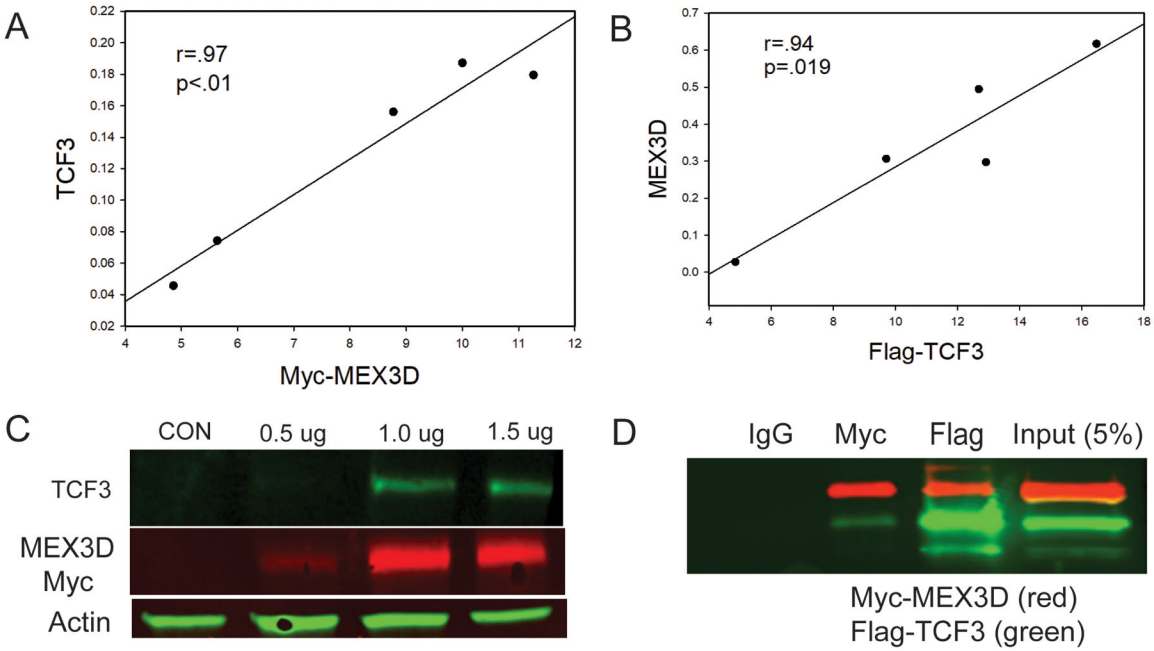

Figure 5. Co-induction and interaction of MEX3D and TCF3.

A. Induction of TCF3 protein in 293 cells by transfection of Myc-tagged MEX3D. Protein was quantitated after Western blotting using Li-Cor software. Correlation coefficient and p value by Pearson Product Moment is shown (r=.97; p<.01)

B. Induction of MEX3D protein in 293 cells by transfection of Flag-tagged TCF3. Protein was quantitated after Western blotting using Li-Cor software. Protein was quantitated after Western blotting using Li-Cor software. Correlation coefficient and p value by Pearson Product Moment is shown (r=.94; p=.019)

C. Induction of TCF3 protein in VCaP cells by transfection of myc-tagged MEX3D using indicated amounts of MEX3D vector DNA or 0.5 ug of empty vector control. Western blot with anti-TCF3 and anti-Myc antibodies. Actin is a loading control.

D. Co-immunoprecipitation of Myc-tagged MEX3D and Flag-tagged TCF3 from protein lysates after cotransfection into 293 cells. IgG: control immunoprecipitation; Myc: anti-Myc antibody immunoprecipitation; Flag: anti-Flag antibody; Input: 5% of input for immunoprecipitation.

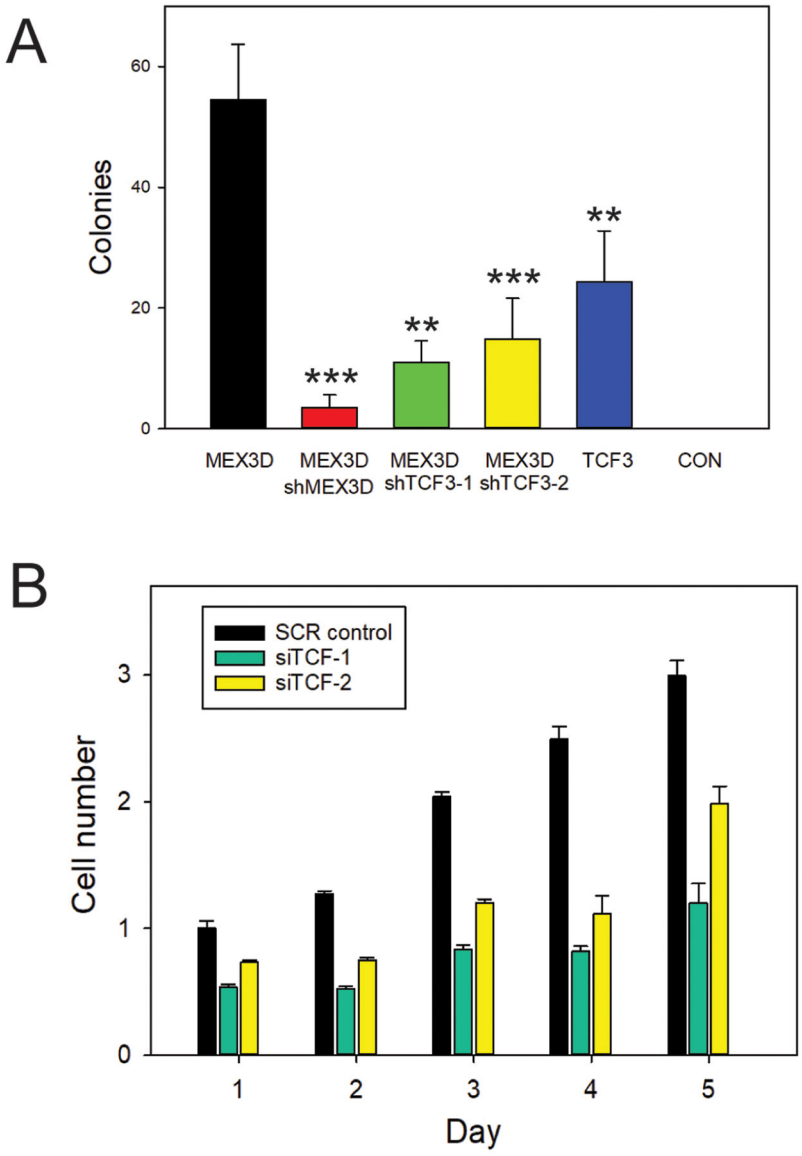

Figure 6. TCF3 has oncogenic activity in prostate epithelial cells

A. Soft agar colony formation was assessed in PNT1A immortalized prostatic epithelial cells overexpressing MEX3D and these same cells with knockdown of MEX3D or TCF3. PNT1A overexpressing TCF3 promoted formation of colonies in soft agar while vector controls formed no colonies as expected. Mean +/− SD. ** p<.01; *** p<.001; One way ANOVA on Ranks versus MEX3D

B. Invasion through Matrigel was assessed in PNT1A immortalized prostatic epithelial cells overexpressing MEX3D and these same cells with knockdown of TCF3 by two different siRNAs or scrambled control. Numbers of invasive cells; Mean +/− SD. All siTCF decreased versus scrambled control on same day, p<.001, t-test